ACS central science

http://pubs.acs.org/journal/acscii

Research Article

MOrPH-PhD: An Integrated Phage Display Platform for the Discovery of Functional Genetically Encoded Peptide Macrocycles

Andrew E. Owens,[†] Jacob A. Iannuzzelli,[†] Yu Gu, and Rudi Fasan*

Cite This: *ACS Cent. Sci.* 2020, 6, 368−381

Read Online

ACCESS | Metrics & More | Article Recommendations | Supporting Information

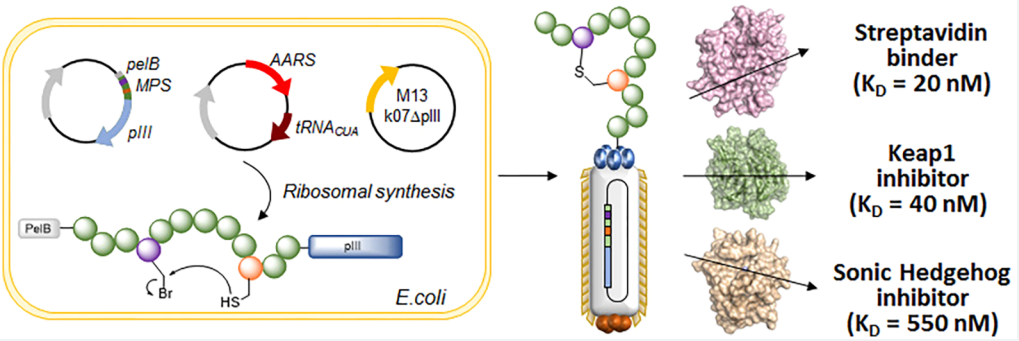

ABSTRACT: Macrocyclic peptides represent attractive scaffolds for targeting protein−protein interactions, making methods for the diversification and functional selection of these molecules highly valuable for molecular discovery purposes. Here, we report the development of a novel strategy for the generation and high-throughput screening of combinatorial libraries of macrocyclic peptides constrained by a nonreducible thioether bridge. In this system, spontaneous, posttranslational peptide cyclization by means of a cysteine-reactive noncanonical amino acid was integrated with M13 bacteriophage display, enabling the creation of genetically encoded macrocyclic peptide libraries displayed on phage particles. This platform, named MOrPH-PhD, was successfully applied to produce and screen 10^5- to 10^8-member libraries of peptide macrocycles against three different protein targets, resulting in the discovery of a high-affinity binder for streptavidin (K_D: 20 nM) and potent inhibitors of the therapeutically relevant proteins Kelch-like ECH-associated protein 1 (K_D: 40 nM) and Sonic Hedgehog (K_D: 550 nM). This work introduces and validates an efficient and general platform for the discovery and evolution of functional, conformationally constrained macrocyclic peptides useful for targeting proteins and protein-mediated interactions.

INTRODUCTION

Macrocyclic peptides have emerged as a valuable class of molecules for the investigation and modulation of protein−protein interactions (PPIs).[1−6] By virtue of their midrange molecular weight (800−3000 Da) and conformational rigidity, macrocyclic peptides have the potential to interact with large, shallow protein surfaces with high affinity and selectivity.[7,8] Furthermore, cyclic peptides often exhibit distinct advantages over their linear counterparts, such as increased proteolytic resistance[9−12] and improved cell permeability,[13−20] which contribute to their value and utility as chemical probes and potential leads for therapeutic development.

Given the increasing importance of macrocyclic peptides as research tools and potential therapeutics, methods for generating and exploring combinatorial libraries of these molecules have become particularly valuable.[21−29] Over the past years, phage display,[21,30−34] mRNA display,[23,35−37] RAPID,[20,27,38,39] and split intein-mediated peptide circularization (SICLOPPS)[40−43] have been successfully applied for the high-throughput screening and affinity selection of cyclic peptide binders of proteins and enzymes. M13 phage display constitutes a particularly powerful and versatile technique for the creation of large (up to 10^9 members) combinatorial libraries of genetically encoded polypeptides and the enrichment of peptide ligands for a protein of interest.[21,22,30] The application of this technique in combination with randomized peptide sequences flanked by two cysteine residues has enabled the identification of disulfide-bridged peptides capable of disrupting protein−protein interactions.[44−49] Unfortunately, the instability of disulfide bonds, in particular under reducing conditions such as the intracellular milieu, limits the utility of these compounds beyond *in vitro* applications or imposes the need for their further modification to overcome these limitations.[50,51] As an alternative approach, chemical cross-

Received: September 14, 2019
Published: February 4, 2020

https://dx.doi.org/10.1021/acscentsci.9b00927
ACS Cent. Sci. 2020, 6, 368−381

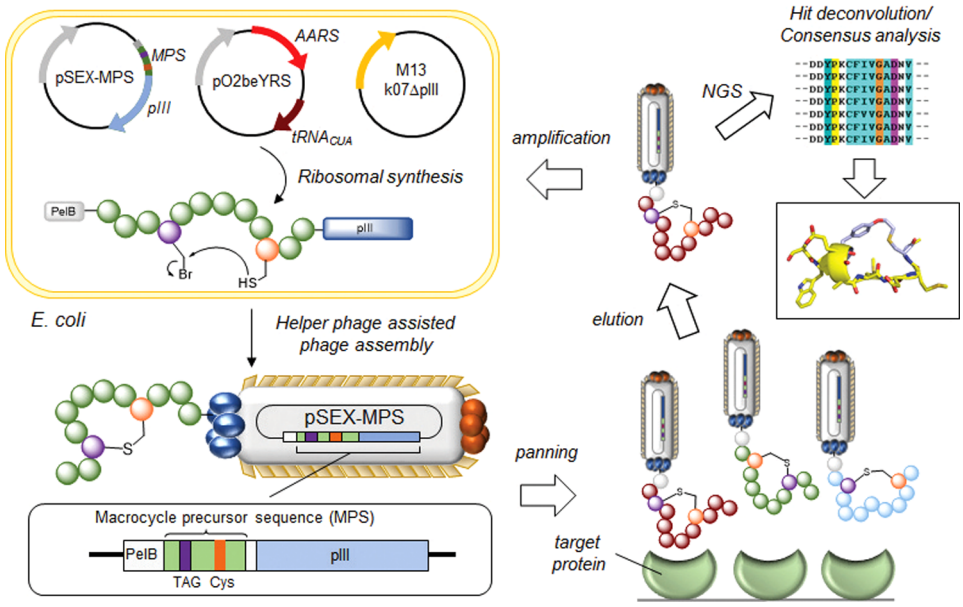

Figure 1. Overview MOrPH phage display (MOrPH-PhD) system. A macrocycle precursor sequence (MPS) is fused to the N-terminal end of the M13 pIII protein encoded by a pSEX-based phagemid vector. Spontaneous, posttranslational peptide cyclization is mediated by the cysteine-reactive O2beY introduced via amber stop codon suppression with an orthogonal AARS/tRNA pair. Phage production in the presence of a helper phage results in M13 phage particles displaying the thioether-bridged macrocycles on the pIII coat protein. The phage-displayed peptide macrocycle library is panned and enriched against an immobilized target, followed by hit deconvolution via DNA sequencing of the MPS encoding gene contained in the bacteriophage.

linking of linear peptide sequences displayed on phage particles has provided an efficient means to obtain (bi)cyclic peptide ligands against a protein/enzyme of interest.[24,52−56] For example, this approach was successfully applied by Heinis and co-workers to discover potent and selective bicyclic peptide inhibitors of human plasma kallikrein and other proteases.[52−55] This method however requires chemical modification of the phage-encoded peptides which can affect the viability and/or infectivity of the phages. More recently, the production of lanthipeptides displayed on phage has been achieved through the coexpression of a lanthipeptide precursor sequence and the corresponding maturation enzymes in a phage-producing host.[29,57] This approach was successfully applied to produce and screen libraries of lanthipeptide analogues, but its scope remains limited to peptide sequences that are recognized and amenable to efficient posttranslational processing by the biosynthetic enzymes. Thus, alternative and potentially general methods for the phage display and functional selection of genetically encoded peptide macrocycles would be highly desirable.

In efforts toward developing strategies for the combinatorial generation of genetically encoded peptide macrocycles, our group has previously introduced methodologies to access peptide-based macrocycles (a.k.a., macrocyclic organo-peptide hybrids or MOrPHs) through the cyclization of ribosomally derived polypeptides by means of genetically encoded noncanonical amino acids (ncAAs).[58−62] In particular, one such method involves a chemo- and regioselective reaction between the cysteine-reactive noncanonical amino acid *O*-(2-bromoethyl)-tyrosine (O2beY) and a proximal cysteine residue, resulting in the formation of macrocyclic peptides constrained by a nonreducible, inter-side-chain-to-side-chain thioether linkage.[61,62] This methodology was recently combined with a low-throughout, plate-based assay to develop a macrocyclic peptide inhibitor of the Sonic Hedgehog/Patched 1 interaction.[63] Here, we demonstrate the successful integration of ncAA-mediated peptide cyclization with M13 phage display to implement a high-throughput platform for the combinatorial synthesis and functional exploration of large libraries of genetically encoded macrocyclic peptides. This methodology was validated through the discovery of a high-affinity binder for streptavidin and potent macrocyclic peptide inhibitors of Sonic Hedgehog and Keap1, demonstrating its value toward the discovery and evolution of macrocyclic peptides capable of targeting proteins and protein-mediated interactions.

RESULTS AND DISCUSSION

Design of MOrPH Phage Display System (MOrPH-PhD). The envisioned strategy for the generation and functional screening of thioether-bridged macrocyclic peptides displayed on M13 bacteriophage is schematically described in Figure 1. To implement this method, we selected to adapt the Hyperphage system[64] to our purpose, as this system was previously reported to facilitate the phage display of complex polypeptides,[65,66] also encompassing noncanonical amino acids.[67,68] As shown in Figure 1, the present MOrPH-PhD system was designed to feature a cyclic peptide genetically fused to the N-terminus of the M13 phage coat protein pIII, which is present in five copies on the tip of the phage particle. To achieve this, a macrocycle precursor sequence (MPS) is inserted between a pelB leader sequence and the pIII coat protein in a phagemid (pSEX81) vector which contains an intergenic region (IGR) for packaging into the phage particle but lacks the remainder of the M13 phage genes. The pelB signal sequence is required for directing the cargo polypeptide to the periplasmic space of *E. coli*, where it is proteolytically cleaved by a signal peptidase. The macrocycle precursor sequence consists of a peptide sequence containing a cysteine residue and the noncanonical amino acid O2beY, which is

https://dx.doi.org/10.1021/acscentsci.9b00927
ACS Cent. Sci. 2020, 6, 368−381

genetically incorporated via amber stop codon (TAG) suppression[69,70] using an engineered aminoacyl-tRNA synthetase/$tRNA_{CUA}$ pair[61] derived from *Methanococcus jannaschii* tyrosyl-tRNA synthetase and its cognate tRNA. As established previously, incorporation of O2beY in close proximity to a downstream or upstream cysteine (2−10 residues apart) is sufficient for these residues to undergo a nucleophilic substitution reaction to yield a thioether-bridged macrocyclic peptide.[61] Maturation of the phage particles incorporating the macrocycle−pIII fusions is made possible through infection of the host *Escherichia coli* cell (TOP10F′) with a helper phage, whose genome lacks the pIII gene and the IGR. Since the phagemid is the only source of pIII protein, and the latter is only expressed upon suppression of the amber stop codon with O2beY, this system ensures that (a) only the macrocycle−pIII fusion protein is incorporated into the mature phage particles, and (b) the phagemid vector containing the gene that encodes for the macrocycle precursor sequence is integrated into the phage, thus establishing the required link between phenotype and genotype for library deconvolution. The phage library is then panned against a target of choice, and higher-affinity binders are enriched through multiple rounds of affinity-based selection and amplification, followed by hit deconvolution via DNA sequencing (Figure 1).

Display of O2beY-Containing Sequences on M13 Phage Particles. To assess the feasibility of the strategy outlined above, we set out to first establish the successful incorporation of O2beY in mature M13 phage particles by means of the engineered aminoacyl-tRNA synthetase O2beY-RS. To this end, a phagemid (pSEX81) construct was generated that encodes for an arbitrary linear peptide sequence containing an amber stop codon (TAG) and no cysteines (NB9 = (amber stop)TGSKLAEYG), fused to the N-terminal end of M13 phage coat protein pIII. This construct was then transformed into *E. coli* TOP10F′ cells containing a pEVOL-based plasmid[71] encoding for the O2beY-RS synthetase and the cognate amber suppressor tRNA,[61] followed by infection with M13 K07ΔpIII helper phage. Since O2beY-RS was previously shown to selectively incorporate a noncanonical amino acid structurally similar to O2beY, i.e., *O*-propargyl-tyrosine (OpgY),[61] this ncAA was also used to assess the amber stop codon suppression efficiency of O2beY-RS in the phage-producing *E. coli* cells. Production of the phage in the absence of the noncanonical amino acid was expected to result in a reduced phage titer upon amplification in *E. coli* due to reduced expression of the minor coat protein pIII. Following optimization of the expression conditions, a >1000-fold higher M13 phage titer was eventually obtained in the presence of either ncAA (O2beY or OpgY) compared to identical expression conditions in the absence of it (Figure 2). These results indicated that the amber stop codon had been successfully suppressed with the noncanonical amino acid, leading to the production of full-length, functional pIII. Further control experiments showed that phage titers up to 10^{12} phage forming units (p.f.u.) could be obtained in the presence of amber stop codon suppression with O2beY. While these titers are ca. 10^3-fold lower than that of wild-type M13 produced under identical conditions, they greatly exceed the transformation efficiency of *E. coli*, thus enabling the coverage of large (e.g., up to 10^9) libraries of DNA variants transformed in this host. In addition, the designed system (Figure 1), along with the use of an invariant amber stop codon in the precursor peptide libraries (*vide infra*), eliminates any possible

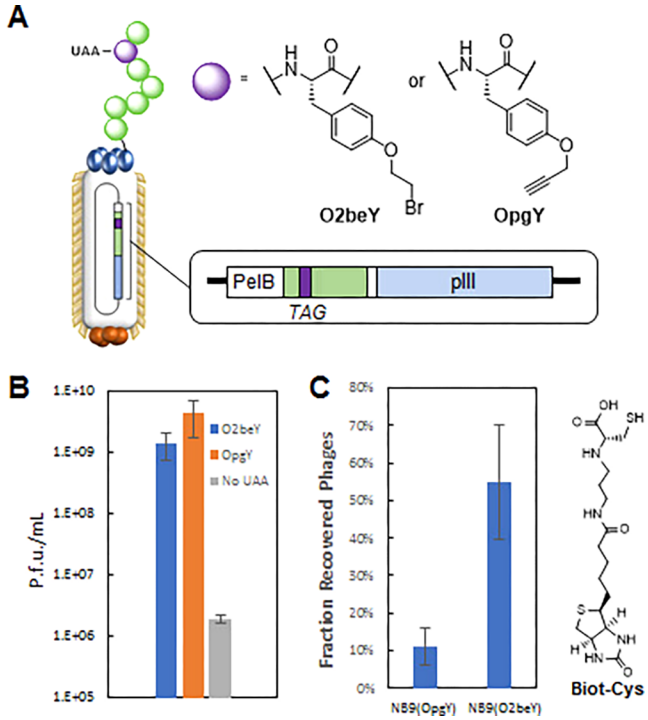

Figure 2. Display of O2beY-containing peptide on M13 phages. (A) Incorporation of cysteine-reactive O2beY and cysteine-unreactive OpgY into a linear nonapeptide (NB9) N-terminally fused to the M13 phage coat protein pIII. (B) Plaque forming units (p.f.u.) generated in the absence and presence of either noncanonical amino acid from *E. coli* cells expressing the polyspecific O2beY-RS synthetase, as determined by the phage titer assay. (C) Selective recovery of O2beY-displaying phages over OpgY-displaying ones using streptavidin-coated beads after phage exposure to biotin-conjugated cysteine reagent (Biot-Cys).

competition from wild-type pIII for incorporation into the phage particles.

To assess whether O2beY maintains an integer side-chain alkyl-bromide group during phage assembly, as required for mediating peptide cyclization, the O2beY-containing phages were incubated with an excess of biotin-conjugated cysteine, followed by pull-down using streptavidin-coated beads. As a negative control, phages displaying the peptide sequence containing OpgY, which is unable to react with thiol nucleophiles, were subjected to the same treatment. As shown in Figure 2C, the phages produced in the presence of O2beY could be recovered from the streptavidin-coated beads at significantly higher levels than the OpgY-containing phages, thus demonstrating the successful incorporation and display of functional O2beY on the phage particles. On the other hand, the subquantitative (∼50%) recovery of the O2beY-containing phages in this experiment was not surprising considering the much slower kinetics for the intermolecular reaction of O2beY with thiol nucleophiles compared to the proximity-driven intramolecular cyclization reaction with cysteine, as established in our previous studies.[61,63]

Affinity Selection of Streptavidin-Binding Macrocyclic Peptides. Encouraged by these results, we set out to assess the functionality of the phage display-based strategy for functional selection of thioether-linked macrocyclic peptides (Figure 1) using streptavidin as a model target protein. To this end, two libraries of macrocyclic peptides displayed on phage were prepared using target sequences in which a fixed HPQ

https://dx.doi.org/10.1021/acscentsci.9b00927
ACS Cent. Sci. 2020, 6, 368−381

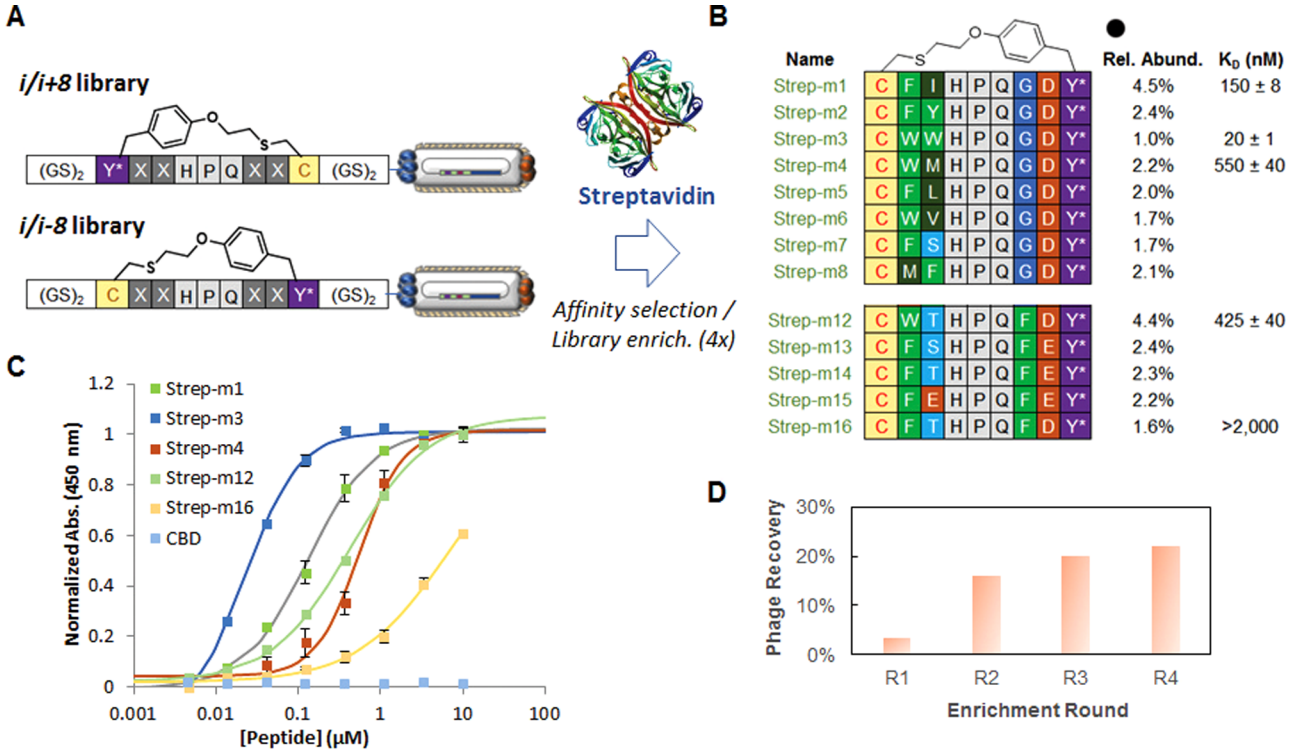

Figure 3. Affinity selection of streptavidin-binding peptide macrocycles. (A) Libraries of semirandomized O2beY-linked peptide macrocycles (X = NNK codon) displayed on phages.(B) Hit sequences identified by deep sequencing (relative abundance = n/54 000 sequences) after library panning against streptavidin-coated magnetic beads. K_D values refer to the corresponding FLAG-macrocycle-CBD constructs in purified form. (C) Binding curves for selected peptide macrocycle hits as determined using a direct binding assay with plate-immobilized streptavidin and HRP-conjugated anti-FLAG antibody for detection of the bound peptide. CBD alone shows no detectable binding to streptavidin. (D) Phage enrichment over the four rounds of affinity selection and amplification as determined via the phage titer assay.

motif is flanked by four fully randomized positions (NNK codon, where N = A, G, C, or T and K = G or T) and the O2beY/Cys pair (Figure 3A). The HPQ motif is a low-affinity (K_D > 100 μM)[72] streptavidin-binding epitope, and it was incorporated into the target sequence to enable benchmarking of the hits isolated using the present system against HPQ-containing peptides previously identified via panning of phage display libraries of disulfide-bridged peptides.[73−75] While encompassing an identical semirandomized sequence, the two macrocyclic peptide libraries differed in the relative arrangement of the O2beY/Cys pair (i/i+8 and i/i−8, where i is O2beY), providing a means to assess the effect of the thioether linkage orientation on the outcome of the affinity selection experiments. After production in *E. coli* (2×10^7 colony forming units (c.f.u.); total size of DNA library, 2.2×10^6), the two phage-displayed macrocycle libraries were panned against streptavidin immobilized on resin beads and subjected to four rounds of enrichment and amplification with increasing stringency and competitive elution with biotin (Figure 3D). Upon deep sequencing of the enriched library after the final round of affinity selection, a clear consensus was observed revealing two major families of peptide sequences with a Cys/O2beY (i/i−8) connectivity (Figure 3B). Specifically, the enriched sequences showed a strong preference for aromatic (Trp, Phe, Tyr) and hydrophobic residues (Met, Ile, Leu) preceding the HPQ motif and a Gly/Asp or Phe/(Glu/Asp) diad following the HPQ sequence (Figure 3B). Interestingly, none of the members from the O2beY/Cys-linked (i/i+8) macrocycle library were enriched during the panning experiments, indicating that this cyclization geometry yielded lower-affinity binders for streptavidin compared to those populating the i/i−8 library.

Based on the sequencing results, selected hits from the panning experiments against streptavidin were chosen for further validation using a streptavidin-binding assay. To this end, three peptide sequences from the "−GD" family and two from the "−FD" family, respectively, were subcloned into a pET22 vector for expression of the corresponding macrocyclic peptides fused to a N-terminal FLAG tag and a C-terminal chitin binding domain (CBD) and polyhistidine tag to facilitate purification and quantification. These constructs were recombinantly produced in *E. coli* using the O2beY-specific amber stop codon suppression system. After purification, each construct was found to have undergone quantitative cyclization (>99%) as determined by MALDI-TOF mass spectrometry (Figure S1). The purified FLAG-tagged macrocycles were then evaluated for their binding affinity to streptavidin in a plate-based assay, in which plate-immobilized streptavidin is exposed to varying concentrations of the macrocycle, and the amount of streptavidin-bound peptide is quantified colorimetrically using a horseradish peroxidase (HRP)-conjugated anti-FLAG antibody (Figure 3C). Importantly, the majority of the tested macrocycles (4/5) were found to bind streptavidin with high affinity, exhibiting a binding dissociation constant (K_D) ranging from 20 to 550 nM (Figure 3B). A control FLAG-tagged CBD construct lacking any target peptide sequence showed no detectable binding to streptavidin, ruling out any contribution to binding from the CBD tag (Figure 3C). In this assay, the best streptavidin-binding peptide, Strep-m3, was found to bind streptavidin with

https://dx.doi.org/10.1021/acscentsci.9b00927
ACS Cent. Sci. 2020, 6, 368−381

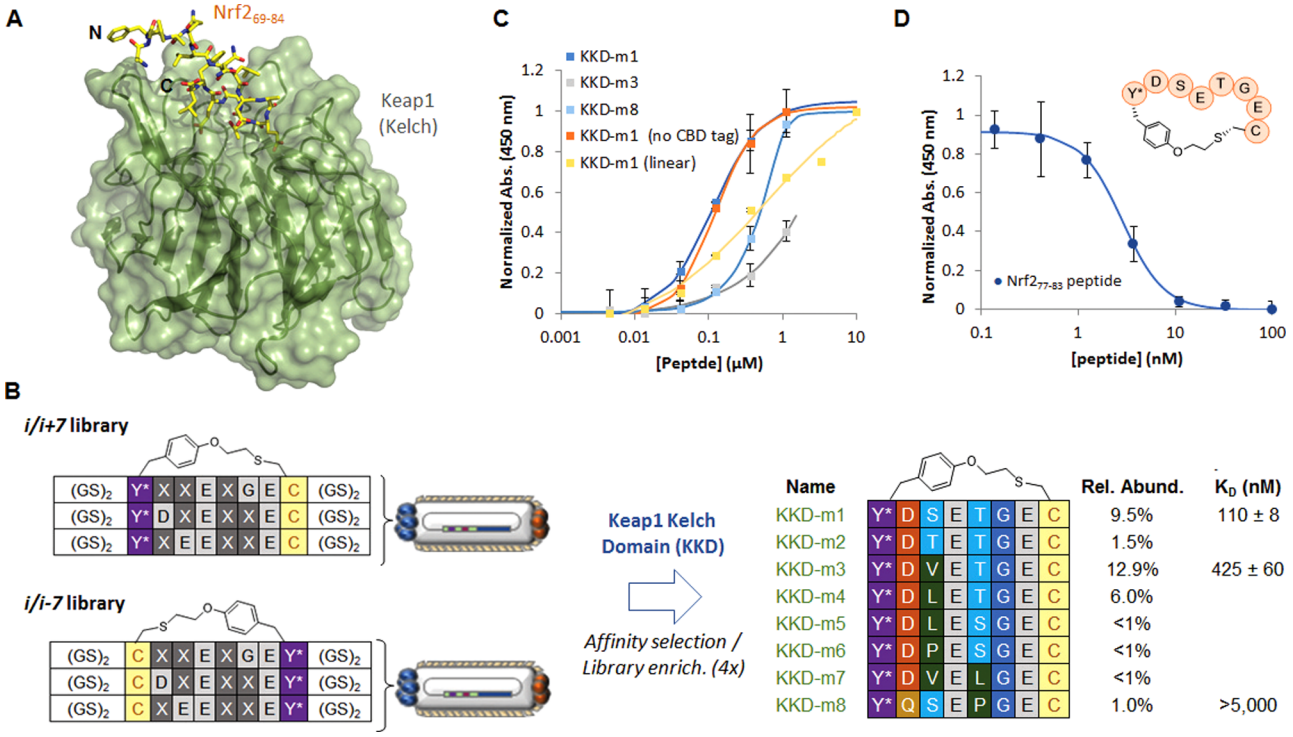

Figure 4. Identification of macrocyclic peptide inhibitors of Keap1/Nrf2 interaction. (A) Crystal structure of Keap1 Kelch domain (KKD) in complex with the Nrf2 regulatory domain (pdb 2FLU).[83] (B) Libraries of semirandomized O2beY-linked peptide macrocycles (X = NNK codon) displayed on phages and hit sequences identified by deep sequencing (relative abundance = n/56 000 sequences) after library panning against immobilized KKD. K_D values correspond to the FLAG-tagged CBD-fused peptide macrocycles. (C) Binding curves for selected macrocyclic peptides as determined using a direct binding assay with plate-immobilized KKD and HRP-conjugated anti-FLAG antibody for detection of the bound peptide. (D) Competition assay in which binding of FLAG-KKD-m1 to immobilized KKD is inhibited by a Nrf2-derived peptide (IC_{50} = 2.8 ± 0.1 nM).

a K_D of 20 nM. In contrast, a linear counterpart obtained by replacing O2beY with the structural analogue OpgY showed a 2-fold weaker binding affinity, highlighting a beneficial effect of the cyclic backbone. Furthermore, the cyclic peptide Strep-m3 could be proteolytically cleaved from the CBD tag using a preinstalled Factor Xa cleavage site, followed by HPLC purification and MS characterization (Figure S1). The purified macrocyclic peptide showed a binding affinity for streptavidin comparable to the CBD-fused peptide, confirming the specificity of the interaction between the targeted protein and cyclic peptide. Altogether, these experiments provided an initial validation of the functionality of the MOrPH-PhD system for the isolation of macrocyclic peptide binders to a target protein.

Discovery of Macrocyclic Peptides Inhibitors of the Keap1/Nrf2 Interaction. Based on these promising results, we sought to assess the utility of this platform for the discovery of functional macrocyclic peptides against biomedically relevant protein targets. To this end, we chose to target the Kelch-like ECH-associated protein 1 (Keap1), which is implicated in sequestration and ubiquitination of Nrf2, a transcriptional regulator that promotes the expression of genes that exert a cytoprotective function in response to oxidative stress and reactive (electrophilic) chemicals in human cells.[76−78] Disruption of the Nrf2/Keap1 interaction has been identified as a promising target for upregulating the expression of cytoprotective oxidative stress response enzymes for anti-inflammatory therapy[79,80] in the context of diabetes[81] and neurodegenerative diseases.[82] The available X-ray crystal structure of the complex between the β-propeller Kelch domain of Keap1 (KKD) and a 16mer Nrf2-derived peptide ($Nrf2_{69-84}$) shows that the Nrf2-derived peptide binds in a shallow pocket on the top face of Keap1 Kelch domain (Figure 4A).[83] These studies further revealed that two glutamate residues in the Nrf2-derived peptide, Glu79 and Glu82, make energetically important interactions with the Kelch domain of Keap1 by establishing a network of hydrogen bonds with nearby residues in the bound protein (Figure S6).[83] Based on this information, two sets of phage display libraries were designed for the purpose of developing macrocyclic inhibitors of the Keap1/Nrf2 interaction. Both sets of libraries were based on a i/i+7 cyclized peptide containing two fixed Glu residues (i.e., E4 and E7) in a i/i+3 arrangement, as for Glu79/Glu82 in the Nrf2 peptide, flanked by three fully randomized residue positions (NNK) in various combinations. Also, both orientations of the O2beY-mediated thioether linkage, i.e., via a i/i+7 connectivity using O2beY1/Cys8 and a i/i−7 connectivity using Cys1/O2beY8, were explored to further diversify the library (Figure 4B).

The resulting phage display libraries (DNA library size: 2.0 × 10^5, comprising 5 × 10^4 unique peptide sequences) were subjected to four rounds of affinity selection against the Keap1 Kelch domain immobilized on plate, followed by deep sequencing of the enriched clones. These analyses showed a significant enrichment only for members of the i/i+7-linked macrocycle library, indicating that this connectivity results in significantly better binders to Keap1 as compared to the i/i−7-linked macrocycles. Furthermore, a strong consensus sequence was observed across the identified hits, which could be clustered into two major sequence families corresponding to

https://dx.doi.org/10.1021/acscentsci.9b00927
ACS Cent. Sci. 2020, 6, 368−381

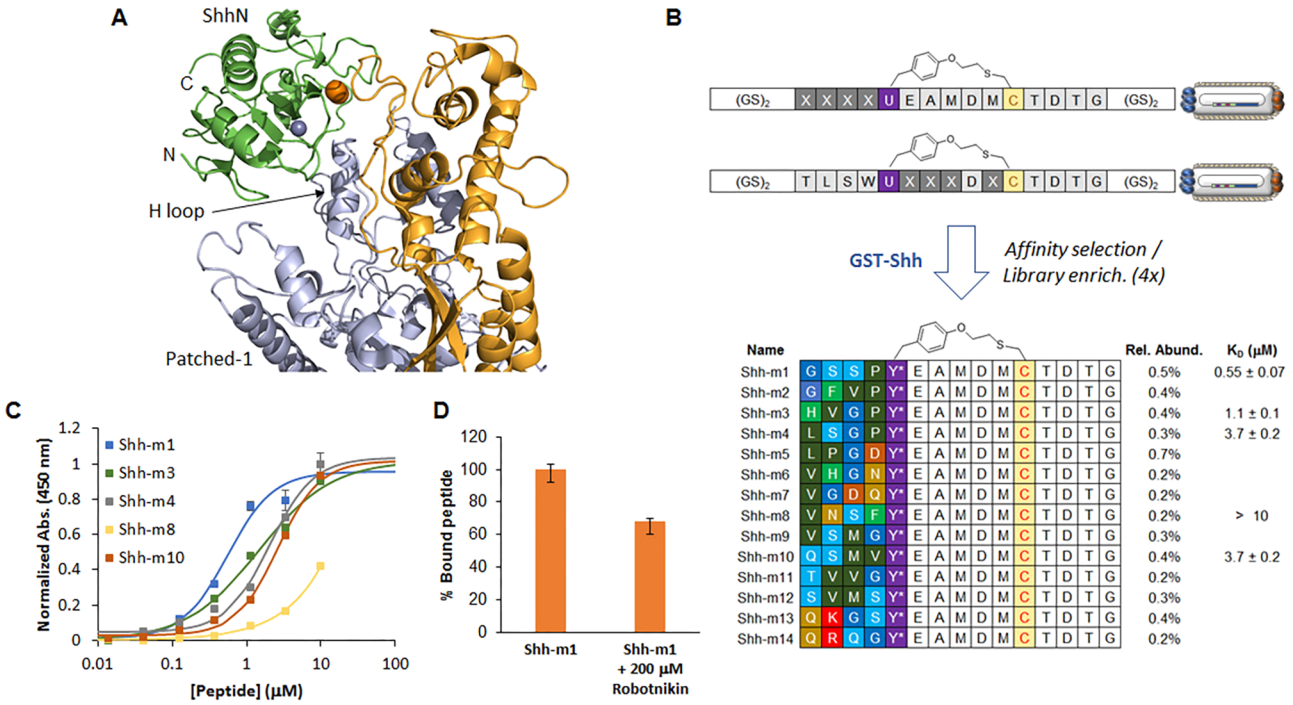

Figure 5. Isolation of macrocyclic peptide inhibitors of Sonic Hedgehog (Shh) signaling protein. (A) Cryo-EM structure of Patched-1 (extracellular domains) in complex with N-terminal domain of Sonic Hedgehog (ShhN) (pdb 6DMY).[97] The Shh binding motif (H loop) mimicked by the L2 loop in HHIP (Figure S7) is highlighted. (B) Libraries of *i*/*i*+6-linked macrocycles based on the HHIP L2 loop (Figure S7; X = NNK) and enriched sequences after library panning against immobilized Shh with respective to relative abundance (=*n*/44 000) and K_D values. (C) Binding curves for macrocyclic Shh-binding peptides as determined using an ELISA assay with immobilized Shh and HRP-conjugated anti-FLAG mAb. (D) Relative Shh binding response for Shh-m1 (1 μM) in the absence and presence of 200 μM robotnikinin.

(**O2beY**)D(S/T)ETGEC and (**O2beY**)D(Φ)E(T/S)GEC (Figure 4B).

The most highly enriched macrocycles from each of the two families of consensus sequences (KKD-m1 and KKD-m3), along with a representative member of a less abundant family (KKD-m8), were then produced recombinantly in *E. coli* fused to a N-terminal FLAG tag and a C-terminal CBD tag for ease of detection and purification. After isolation, cyclization of these target sequences was confirmed via MALDI-TOF MS analysis (Figure S2). The purified FLAG-tagged cyclic peptides were then tested for their ability to bind the Keap1 Kelch domain (KKD) using an *in vitro* assay, in which peptide binding to plate-immobilized KKD is detected via an HRP-conjugated anti-FLAG antibody (Figure 4C). Gratifyingly, these experiments showed that all of the tested macrocycles interact with Keap1 with high (sub-micromolar) affinity, with the most promising compound (KKD-m1) binding Keap1 with a K_D of 110 nM (Figure 4B). A nearly identical binding affinity (K_D: 120 ± 10 nM) was measured for this macrocyclic peptide after proteolytic cleavage of the CBD tag (Figure S2), indicating the lack of contributions from the purification tag to Keap1 binding. In addition, a linear version of the same peptide, prepared by substituting O2beY with OpgY, was found to bind Keap1 with a 5-fold lower affinity (K_D = 555 ± 17 nM), highlighting the importance of the cyclized structure for optimal interaction with the target protein.

The isolated KKD-m1 macrocycle was then further investigated to assess its ability to block the interaction of Keap1 interaction with Nrf2. To this end, a competition assay was used in which immobilized Keap1 was incubated with the FLAG-tagged macrocycle and increasing amounts of a Nrf2-derived peptide encompassing the Keap1-binding region ($Nrf2_{77-83}$).[84] These experiments showed that the Nrf2-derived peptide is able to inhibit Keap1-m1 binding to Keap1 (IC_{50} = 2.8 nM; Figure 4D), indicating that the two peptides interact with the same binding site on the Keap1 protein.

Macrocyclic Peptide Inhibitors of Sonic Hedgehog. Next, we wished to investigate the utility of the phage display platform toward the discovery of macrocyclic peptide inhibitors of Sonic Hedgehog (Shh), a key signaling protein implicated in the activation of the Hedgehog pathway.[85−87] The Hedgehog pathway plays a critical role in controlling embryonic development, and its abnormal activation has been implicated in various human malignancies, including leukemia and tumors of the prostate, pancreas, and colon.[88,89] This signaling pathway is initiated by the interaction of Shh with the extracellular domain of the transmembrane receptor Patched-1 (PTCH1),[90] which triggers a signal transduction cascade resulting in the transcription of the Hedgehog pathway target genes.[91−93] Recently, our group developed a macrocyclic inhibitor of the Shh/Patched interaction, called HL2-m5,[63] through cyclization and optimization of a peptide sequence derived from a Shh-binding loop found in Hedgehog Interacting Protein (HHIP),[94,95] a natural negative regulator of the Hedgehog pathway.[96] Here, we sought to leverage the present phage display system to explore and identify alternative macrocyclic peptides for targeting this therapeutically important protein−protein interaction.

To this end, a phage display macrocycle library was generated based on the sequence encompassing the L2 loop in HHIP ($HHIP_{376-387}$: TLDDMEEMDGLSD). Crystallographic analyses showed that this structural motif binds to a shallow cleft on the Shh surface (Figure S7),[94,95] which

https://dx.doi.org/10.1021/acscentsci.9b00927
ACS Cent. Sci. 2020, 6, 368−381

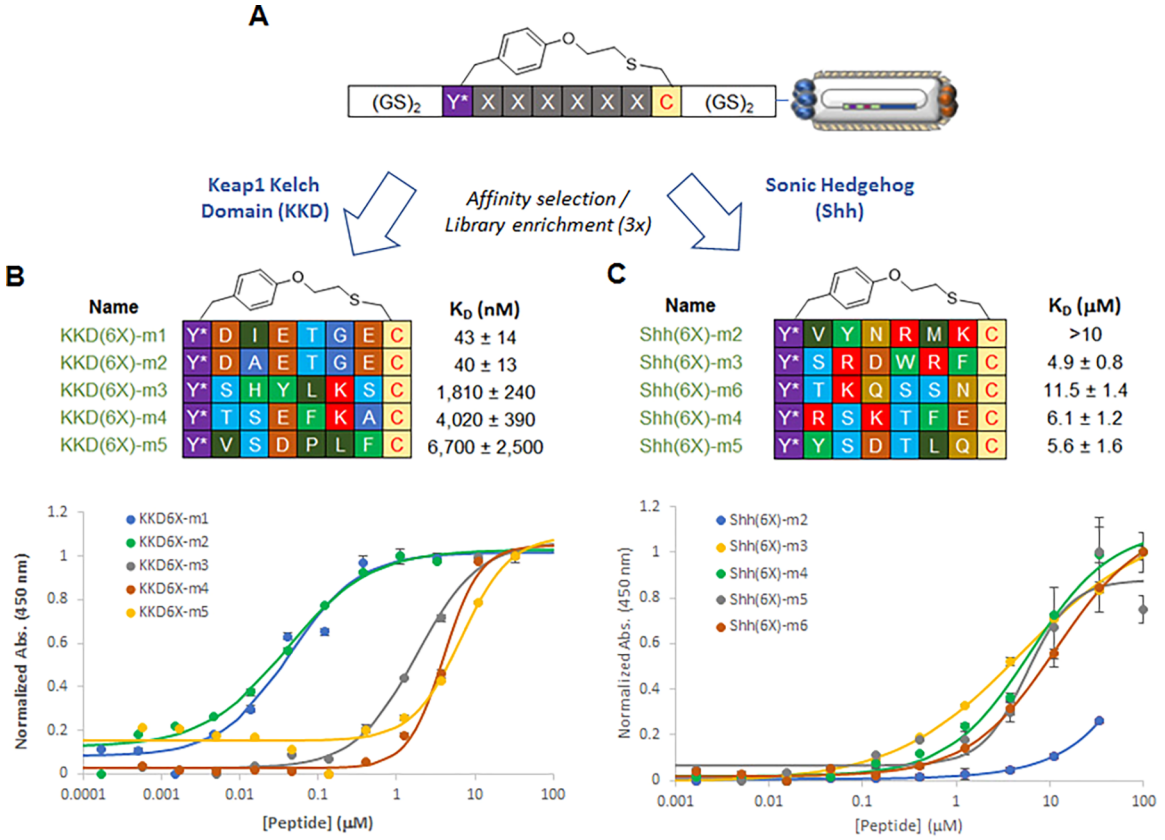

Figure 6. Keap1 and Sonic Hedgehog (Shh) binding macrocyclic peptides from the naïve MOrPH-PhD library. (A) Composition of *i*/*i*+6-linked library (X = NNK; Y* = O2beY). (B) Sequences, binding affinity, and binding curves for selected macrocyclic Keap1-binding peptides isolated after panning the MOrPH-PhD library against immobilized Keap1. (C) Sequences, binding affinity, and binding curves for selected macrocyclic Shh-binding peptides isolated after panning the MOrPH-PhD library against immobilized Shh.

represents a key binding site also for the interaction of an analogous loop motif in Patched-1 (Figure 5A),[97,98] thus defining a mechanism for HHIP-mediated suppression of Hedgehog signaling. While linear HHIP L2-derived peptides exhibit only modest affinity for Shh (K_D ∼ 150 μM),[94] our previous studies[63] suggested that this Shh recognition motif sequence could serve as a starting point for the development of cyclopeptide inhibitors of the Shh/Patched interaction. Accordingly, a library of pIII-fused peptide macrocycles was prepared based on a sequence encompassing the HHIP L2 motif and cyclized via a *i*/*i*+6 thioether linkage through the installation of a O2beY/Cys pair in correspondence to residue Met379 and Leu385 (Figure S7). The sequence was diversified through full randomization (NNK) of four positions within either the N-terminal or central region of the macrocycle (Figure 5B), yielding a DNA library size of ∼2×10^6 members and comprising a total of 3.2×10^5 unique peptide sequences.

The phage-displayed macrocycle library was panned against plate-immobilized Shh and enriched over four rounds of affinity selection and amplification. Next-generation sequencing of the library members isolated after this process revealed a large predominance of sequences derived from randomization of the N-terminal region of the macrocycle (Figure 5B), indicating that no strong benefits for the interaction with Shh derived from variation of the central region of the cyclic peptide. Despite a relatively weak consensus emerging from the isolated hits, two major groups of related sequences could be identified which share a Pro residue at position 4 (Shh-m1 through Shh-m4) and/or a Leu/Val residue at position 1 (Shh-m4 through Shh-m9). While a relatively larger variation was observed for the other randomized sites, a predominance of Gly and polar residues (Ser, Asn, Gln) was apparent at these positions. Five representative members of the pool of sequences were then expressed and purified in GyrA-fused form, and the FLAG-tagged macrocycles were isolated via thiol-induced cleavage of the GyrA intein. Characterization by MALDI-TOF MS confirmed the quantitative occurrence of O2beY-mediated cyclization, as judged based on the absence of acyclic side products or other adducts (Figure S3). The Shh binding affinity of the macrocycles was then assessed using a binding assay analogous to that used for the other target proteins. From these experiments, most of the tested macrocyclic peptides were found to be able to bind Shh with low micromolar to sub-micromolar affinity (Figure 5C). Among these, Shh-m1 emerged as the most promising hit, exhibiting a K_D for Shh binding of 550 nM (Figure 5B). While this peptide is a weaker Shh binder than the previously reported HL2-m5 (K_D = 170 nM),[63] a cyclic version of the HHIP L2 sequence binds Shh with a nearly 7-fold lower affinity (K_D = 3.6 μM) compared to Shh-m1. Thus, in addition to confirming the beneficial effect of the mutations found in Shh-m1 for interaction with Shh, these results demonstrate the ability of the present platform to favor the selection of functional binders for this target protein. To further assess the ability of the macrocyclic peptide to act as an inhibitor of Shh function, a competition assay was carried out in the presence of robotnikinin, a known small-molecule inhibitor of Shh (K_D = 3.1 μM).[99] Upon incubation in the presence of high

https://dx.doi.org/10.1021/acscentsci.9b00927
ACS Cent. Sci. 2020, 6, 368−381

concentrations of robotnikinin (200 μM), Shh-m1 binding to Shh was reduced by approximately 40% (Figure 5D), confirming that this macrocyclic peptide interacts with the region of Shh targeted by robotnikinin and implicated in Patched activation.[99]

Keap1- and Shh-Targeting Peptide Macrocycles from Naïve MOrPH-PhD Library. Having demonstrated the functionality of the MOrPH-PhD system for the screening of medium-size cyclopeptide libraries (i.e., up to 10^5 members), we sought to assess the efficiency of this platform toward enabling the discovery of functional cyclopeptides from a larger, naïve library of peptide macrocycles. To this end, we generated a MOrPH library with a fully randomized (NNK) hexamer sequence in the format O2beY-$(Xaa)_6$-Cys, which encompasses a billion-member gene library and ~10^8 unique peptide sequences. The corresponding MOrPH-PhD library was panned, in parallel, against immobilized Keap1 and Shh via three rounds of affinity selection and phage amplification (Figure 6). After sequencing, five representative members of the recovered sequences were produced recombinantly and tested for their affinity toward the corresponding target protein using the binding assays described earlier. All of the chosen sequences were found capable of generating the expected macrocyclic peptide as determined by MALDI-TOF mass spectrometry (Figures S4 and S5). As summarized in Figure 6B, all of the hits isolated from the Keap1 selection experiments were found to be viable binders of this protein, showing low micromolar to low nanomolar affinity toward it. Notably, the best performing peptides within this group, KKD(6X)-m1 and KKD(6X)-m2, interact with Keap1 with a K_D of 40 nM, which corresponds to a nearly 3-fold higher affinity than the best Keap1 binder isolated from the Glu/Glu motif-based library (KKD-m1, K_D = 110 nM; Figure 4B). Interestingly, the best hits from the naïve library (KKD(6X)-m1 and KKD(6X)-m2, Figure 6B) share a high sequence similarity with the best hits from the semirandomized library (KKD-m1 and KKD-m2, Figure 4B), thus denoting a strong convergence of the two independent libraries and affinity selection experiments toward a common consensus sequence. The other peptides, which share common features among each other but are otherwise sequence-unrelated to KKD(6X)-m1, were determined to bind Keap1 with a binding affinity in the low micromolar range. Among them, the best compound is KKD(6X)-m3 with a K_D of 1.8 μM (Figure 6B).

Panning of the same MOrPH-PhD library against Shh led to the selection of a different set of peptide sequences, most of which (5/6) proved to be viable Shh binders in the *in vitro* assay (Figure 6C). Among them, the best binders were determined to be Shh(6X)-m3 and Shh(6X)-m5, which show low micromolar affinity toward interaction with Shh (K_D = 4.9−5.6 mM). These peptides feature a distinct amino acid sequence compared to each other and compared to the best hit peptide isolated from the HHIP L2 loop-based library (Figure 5B). Interestingly, despite these structural differences, they both incorporate an Asp residue in the central part of their sequence, which may potentially mimic the function of an energetically important Asp residue mediating the interaction between HHIP and a Zn(II) ion in the binding cleft of Shh (Figure S7).

DISCUSSION

In this work, we have described the successful implementation and application of an M13 bacteriophage-based platform for the display and selection of thioether-bridged macrocyclic peptides. This system enables the exploration of combinatorial libraries of genetically encoded cyclic peptides of arbitrary sequence and constrained by a stable (i.e., nonreducible) linkage. Using this system, we were able to successfully identify high-affinity binders and inhibitors (K_D: 20−230 nM) for three different target proteins, namely, streptavidin, Keap1, and Sonic Hedgehog. As such, these results demonstrate the functionality and versatility of the present MOrPH-PhD strategy for discovering macrocyclic peptides capable of targeting a panel of structurally diverse proteins.

The binding affinity of the best streptavidin-binding cyclopeptide identified here (K_D: 20 nM) is 10- to 30-fold higher than those of streptavidin binders previously isolated through the panning disulfide-bridged peptide libraries displayed on phage (K_D of 270 and 670 nM for *cyclo*-[CHPQFC] and *cyclo*-[CHPGPPC], respectively).[73−75] At the same time, while reduction of the disulfide bridge in the latter compounds was reported to result in a 70-fold loss of binding affinity for streptavidin, the thioether linkage in Strep-m3 makes it insensitive to reducing conditions, thus denoting another key advantage of the peptide cyclization strategy exploited here.

With Keap1, screening of the naïve macrocyclic peptide library and of the "semirational" library incorporating a $Glu(X)_nGlu$ motif inspired by a dyad of energetically important residues at the Nrf2/Keap1 interface converged into the selection of a potent inhibitor of the Keap1/Nrf2 peptide interaction with a structure corresponding to *cyclo*[Y*D(X)-ETGEC], where Y* is Cys-cross-linked O2beY, and X is Ile, Ala or Ser (i.e., KDD(6X)-m2, KDD(6X)-m1, KDD-m1, respectively). From a methodology standpoint, this strong convergence of two independent libraries and affinity selection experiments to a common consensus sequence provides further validation of the robustness of the MOrPH-PhD platform. Interestingly, the peptide sequence encompassing these macrocycles closely overlaps with that of the tip of Nrf2 β-hairpin inserting into a cleft on Keap1 Kelch domain (...$D^{77}EETGE^{82}$...; Figure 4A),[83] suggesting a potentially similar binding mode for these macrocyclic peptides compared to the Keap1-binding epitope in Nrf2. At the same time, the structure−activity data accrued about the more variable i+2 position in these cyclic peptides (i.e., Ala ≈ Ile > Ser > Val) points at the important role of this residue in modulating binding of the macrocycle to Keap1. On the other hand, by featuring a completely divergent sequence compared to this set of structurally related peptides, KKD(6X)-m3 provides an alternative macrocyclic scaffold for targeting the Nrf2/Keap1 interaction.

Previously, our group developed a sub-micromolar inhibitor of Shh (HL2-m5 = TLSW(Y*)EAMDMCTD, where Y* is Cys-cross-linked O2beY; K_D = 170 nM) through affinity maturation of a HHIP L2-derived cyclic peptide via screening of macrocycle libraries produced in cells and arrayed on multiwell plates.[63] Here, the same L2 loop motif was used as a starting point to develop a set of structurally related cyclopeptides with low to submicromolar Shh binding affinity (Figure 5B) useful for targeting the Shh/Patched interaction. Although the best hit isolated from this library (Shh-m1) is a weaker Shh binder compared to HL2-m5, the present phage display-based platform allowed for an extensive exploration of the sequence space within this macrocyclic scaffold, revealing a low and high tolerance to sequence variations within the

https://dx.doi.org/10.1021/acscentsci.9b00927
ACS Cent. Sci. 2020, 6, 368−381

central and N-terminal region of the macrocycle, respectively, for the interaction with Shh. Importantly, screening of the naïve library yielded a distinct set of Shh binders (K_D: 4.9−6.1 mM) which feature a completely unrelated sequence as well as a more compact structure compared to Shh-m1 (8mer vs 15mer). As such, these compounds is expected to furnish a novel macrocyclic peptide scaffold for targeting the Shh/Patched interaction.

Another noteworthy result from the present studies concerns the importance of the orientation of the thioether linkage, i.e., via O2beY/Cys vs Cys/O2beY arrangement, for modulating the structure and thus the function of the macrocyclic peptide. This aspect becomes evident from the affinity selection experiments with streptavidin and Keap1, in which libraries of macrocyclic peptides featuring identical randomized sequences but inverted thioether linkages were evaluated side-by-side. Indeed, macrocycles constrained by a Cys/O2beY linkage proved to be most effective for targeting streptavidin (Figure 3), while an inverted orientation of the thioether linkage (i.e., O2beY/Cys) was found to be more beneficial for targeting Keap1 (Figure 4). In prior studies, we determined that the orientation of the linkage does not inherently affect the efficiency of O2beY-mediated macrocyclization for target sequences of identical length.[61] The capability to modulate and fine-tune the molecular recognition properties of these cyclic peptides through variation of the ncAA/Cys linkage orientation represents another unique feature of the present system compared to currently available methods useful for the screening of cyclic peptide libraries.[22,24,27] In addition, while remaining accessible by solid-phase peptide synthesis,[63] the macrocyclic peptide hits identified using the present system can be readily produced recombinantly and isolated in purified form for rapid validation and evaluation in downstream functional assays.

CONCLUSIONS

In conclusion, this work introduces an efficient and potentially very general platform for the creation and functional exploration of combinatorial libraries of genetically encoded cyclic peptides. As supported by its successful application to the discovery of potent binders/inhibitors for three different target proteins (streptavidin, Keap1, Sonic Hedgehog), this system is expected to constitute a valuable, new tool for the discovery and evolution of bioactive peptide macrocycles capable of targeting proteins and disrupting protein-mediated interactions with high potency and selectivity. The reliance of this system on the use of a readily accessible reagent (O2beY) and spontaneous O2beY-mediated cyclization, along with the capability to readily modulate the cyclic structure and molecular recognition properties of these cyclic peptides through variation of the position and orientation of the O2beY/Cys linkage, adds to the technical simplicity and versatility of this approach. Given our prior success in generating MOrPHs using different cyclization strategies,[58−62] we also anticipate that the present system will be compatible with the use of other cysteine-reactive ncAAs and other ncAA-mediated peptide cyclization chemistries for the exploration of structurally diverse libraries of peptide macrocycles.

EXPERIMENTAL DETAILS

Cloning of Phage Constructs and Libraries. The PhD libraries were constructed via PCR using pSEX81 (Progen) as the template and the appropriate mutagenizing primers (NNK codon randomization; forward primers 1−12, reverse primer 14; Table S1). The PCR product was cloned into the *Nco* I/*Nhe* I cassette of pSEX81, and the recombinant plasmid libraries were transformed in *E. coli* TOP10F′ electrocompetent cells and selected on 20 cm × 20 cm 2XYT agar plates containing ampicillin (100 μg/mL) and tetracycline (5 mg/L). A colony forming unity (c.f.u.) count exceeding by at least 3-fold the size of the respective DNA library was utilized for all the libraries. Colonies were then collected from the plates, and the plasmid library was isolated using a plasmid midi-prep kit (Qiagen). Control constructs such as pSEX81-NB9T and HL2-cyc were cloned into the *Nco* I/*Nhe* I cassette of pSEX81(Progen) using a similar procedure as described above. The recombinant plasmid was transformed into *E. coli* TOP10F′, selected on 2XYT agar plates containing ampicillin (100 μg/mL) and tetracycline (5 mg/L), and confirmed by DNA sequencing.

Phage Expression and Purification. The pSEX81-based plasmid library (or single plasmid construct) was transformed in TOP10F′ *E. coli* cells containing the plasmid pEVOL-O2beY-RS[61] by electroporation; cells were recovered with SOC media (2% w/v tryptone, 0.5% w/v yeast extract, 10 mM NaCl, 2.5 mM KCl, and 20 mM glucose) and incubated with shaking at 37 °C for 1 h. Cells were then transferred to a 200 mL Erlenmeyer flask containing 20 mL of 2XYT media (1.6% w/v tryptone, 1.0% w/v yeast extract, 8.6 mM NaCl) supplemented with ampicillin (50 mg/L), chloramphenicol (34 mg/L), and tetracycline (5 mg/L). Cell cultures were grown overnight (12−16 h) at 37 °C, and then, cells were recovered by centrifugation (4000*g*). The cell pellet was diluted to an OD_{600} of 0.05 in fresh 2XYT media supplemented with ampicillin (50 mg/L), chloramphenicol (34 mg/L), and tetracycline (5 mg/L) and allowed to reach an OD_{600} of 0.6. A volume equal to 10% of the final phage expression culture volume was infected with Hyperphage (Progen) at an MOI of 20. Hyperphage was allowed to infect the cells for 1 h at 37 °C with shaking (200 rpm), and then, the culture was pelleted by centrifugation (4000*g*). The pellet was resuspended in 2XYT supplemented with ampicillin (50 mg/L), chloramphenicol (34 mg/L), tetracycline (5 mg/L), kanamycin (30 mg/L), arabinose (0.06%), and noncanonical amino acid (2 mM). Cultures were grown for 18 h at 30 °C with shaking (200 rpm) to express the desired library or phage clone. After expression, cell cultures were pelleted by centrifugation (4000*g*). The resulting supernatant was incubated at pH 8.5 for 6 h to facilitate complete cyclization of macrocyclic peptides and then concentrated using an Amicon 30 kDal spin filter to a convenient volume (250−300 μL). The concentrated supernatant was then mixed with 1:4 (v/v) 20% polyethylene glycol buffer (20% polyethylene glycol, 2.5 M NaCl) at 4 °C and incubated overnight. The precipitated phage was pelleted by centrifugation (14 000*g*) for 30 min, and resuspended in 200 μL of PBS (10 mM Na_2HPO_4, 1.8 mM, KH2PO4, 137 mM NaCl, 2.7 mM KCl, pH 7.5). The fully resuspended phage solution was centrifuged (14 000*g*) for an additional 5 min to remove any insoluble cellular debris. The clarified phage solution was purified a second time and then passed through a 0.22 μm filter and stored in PBS pH 7.5 buffer at 4 °C.

Determination of Phage Titer. Aliquots (10 μL) of purified phage solutions were serially diluted in 10-fold dilutions with 2xYT media. A 10 μL portion of each dilution

https://dx.doi.org/10.1021/acscentsci.9b00927
ACS Cent. Sci. 2020, 6, 368−381

is added to 90 μL of exponentially growing *E. coli* TOP10F′ cells (OD_{600} = 0.4−0.6) in Eppendorf tubes. The phage was allowed to infect *E. coli* cells for 1 h at 37 °C with shaking on a desktop thermoblock. A 100 μL portion of phage infected *E. coli* was then spread on 2XYT agar plates containing ampicillin (50 mg/L) and tetracycline (5 mg/L) and grown overnight at 37 °C. The phage titer was determined by counting colony forming units.

Phage Biotinylation Experiment. A pSEX81 plasmid encoding for the NB9 sequence N-terminally fused to pIII was expressed in the presence of O2beY (or OpgY) and purified as described above. Each phage preparation was diluted to a titer of 10^{11} p.f.u. in 100 μL of reaction buffer (50 mM potassium phosphate, 0.5 mM TCEP pH 8.5). Biotin-conjugated cysteine was then added to a final concentration of 2 mM, and the reaction was allowed to proceed for 24 h at room temperature. Phage were buffer exchanged against 50 mM potassium phosphate extensively (5 times) using a 30 KDa cutoff centrifugal concentrator (Amicon) to remove unreacted cystine functionalized biotin from the phage solution. Resulting phage was then diluted to a titer of 10^6 p.f.u. in PBS and incubated with magnetic streptavidin beads for 30 min at room temperature. Beads were separated from the supernatant with magnetic separation, and the fraction of recovered phage was calculated from the phage titer (% recovered phages = ((phage input − phage output)/phage input) × 100).

Selection of Streptavidin-Binding Macrocycles. A 10 μL portion of streptavidin-coated magnetic beads (NEB) was washed 3 times with PBS to remove storage buffer and then incubated in 100 μL of PBS with 0.5% BSA for 2 h at room temperature. The beads were removed from the solution by magnetic separation, washed once with PBS, and then incubated with 100 μL of phage in PBS (typical titer: 10^9−10^{11} p.f.u.). The phage/bead mixture was allowed to incubate with gentle shaking for 1 h at room temperature. The beads were then removed from the solution by magnetic separation and washed 3−5 times with PBS-Tween 20 buffer (0.05% Tween-20). The beads were then suspended in 100 μL of 0.1 mM biotin for 30 min at room temperature. After competitive elution, the beads were removed from the solution by magnetic separation. A 10 μL portion of the eluted phage solution was used to determine the titer of recovered phage. The remaining eluted phage was used to infect 2.5 mL mid log TOP10F′ cells (OD_{600} 0.4−0.6) in 2XYT for 1 h at 37 °C. This culture was then pelleted by centrifugation, resuspended in 5 mL of fresh 2XYT (AMP/TET), and allowed to grow to saturation overnight at 37 °C. The plasmid was extracted from the overnight culture, and the enriched plasmid pool was used to propagate new phage as described above. After four rounds of affinity selection and amplification, the enriched library was analyzed by deep sequencing.

Selection of Keap1 and Shh Binding Macrocycles. For the selection experiments, Keap1 Kelch domain[100] and a construct containing Shh[63] fused to a N-terminal poly-His tag via a TEV protease cleavable linker ("Shh") were immobilized on microtiter plates by incubating 100 μL of protein solution at 4 μM in PBS buffer overnight at 4 °C, followed by blocking with 0.5% bovine serum albumin in PBS for 1.5 h at room temperature. Plates were washed (3 × 150 μL of PBS with 0.5% Tween-20) prior to panning. Before each panning round, a negative selection was performed by preincubation of the library in BSA-blocked plates (for Keap1 binders selections) for 30 min at room temperature or by performing the panning in the presence of 1 μM GST for Shh binders selection. Remaining phage was then transferred to positive selection wells with immobilized Shh (or Keap1) and incubated at room temperature for 1 h. Then, wells were washed 3−5 times with 150 μL of PBS with 0.5% Tween-20, and incubated with 50 μL of elution buffer (0.2 M Glycine-HCl, pH 2.2, 1 mg/mL BSA) for 30 min at room temperature. The elution solution was neutralized with 10 μL of neutralization buffer (1 M Tris-HCl, pH 9.1), and the fraction of recovered phages was determined using the phage titer protocol described above. The remaining phage was used to infect TOP10F′ *E. coli* cells for amplification of the library. For each target, four rounds of affinity selection and amplification were carried out. After isolation of the phagemid, the enriched libraries were analyzed by deep sequencing.

Screening of Naïve Library. Shh and Keap1 were immobilized, and the phage library was expressed and purified as described above. Prior to selection, purified phage containing the naïve macrocyclic peptide library were incubated with 50 μL of immobilized TCEP (tris(2-carboxyethyl) phosphine) for 1 h at room temperature with gentle shaking, followed by incubation at pH 8.5 for 2 h. The phage libraries were precipitated with 1:4 (v/v) 20% polyethylene glycol buffer (20% polyethylene glycol, 2.5 M NaCl) at 4 °C for 2 h. The precipitated phage was pelleted by centrifugation (14 000*g*) for 15 min, and resuspended in 100 μL of PBS (10 mM Na_2HPO_4, 1.8 mM, KH_2PO_4, 137 mM NaCl, 2.7 mM KCl, pH 7.4). Phage libraries (10^{11} p.f.u.) were then incubated with immobilized Shh (or Keap1) at room temperature for 1 h with gentle shaking. Then, the wells were washed 3−5 times with 150 μL of PBS with 0.5% Tween-20, and incubated with 50 μL of elution buffer (0.2 M Glycine-HCl, pH 2.2, 1 mg/mL BSA) for 30 min at room temperature. The elution solution was neutralized with 10 μL of neutralization buffer (1 M Tris-HCl, pH 9.1), and the fraction of recovered phages was determined using the phage titer protocol described above. The remaining phage was used to infect TOP10F′ *E. coli* cells for amplification of the library. Three rounds of affinity selection and amplification were performed, after which the enriched library was analyzed by DNA sequencing.

Recombinant Expression and Isolation of Macrocyclic Peptides. The macrocyclic peptides were produced recombinantly as fusion constructs with an N-terminal FLAG tag (MDYKDDDDKGSGS-) and a C-terminal chitin-binding domain (CBD) or a GyrA intein protein containing a C-terminal polyhistidine tag, according to previously reported procedures.[63] Briefly, genes encoding the desired constructs were amplified by PCR and cloned into the *BamH* I/*Xho* I cassette of a pET22 vector containing a N-terminal FLAG-tag and C-terminal His tag. For the CBD-fusion construct, a Factor Xa cleavage site was introduced between the macrocycle precursor sequence and the CBD tag. The recombinant DNA constructs were transformed in *E. coli* DH5α and selected on LB agar plates supplemented with ampicillin (100 mg/L), followed by DNA sequencing. For expression, the desired plasmid vector was transformed in *E. coli* BL21(DE3) containing pEVOL_O2beYRS and grown overnight in 2xYT media with ampicillin (100 mg/L) and chloramphenicol (34 mg/L). The overnight cultures were used to inoculate new cultures at an OD_{600} of 0.05 and grown at 37 °C until mid log growth (OD_{600} = 0.5), at which point they were transferred to

https://dx.doi.org/10.1021/acscentsci.9b00927
ACS Cent. Sci. 2020, 6, 368−381

27 °C. Cultures were then supplemented with O2beY (or OpgY) at 2 mM and induced with arabinose (0.06% w/v); after an hour, IPTG was added at 1 mM. Cells were grown for 16−18 h at 27 °C and then harvested by centrifugation (4000*g*). Pellets were lysed via sonication and clarified by centrifugation (14 000*g*). The peptide constructs were purified from the lysate using Ni-NTA affinity chromatography as per the manufacturer's instructions and stored in PBS pH 7.5. The macrocyclic peptides were characterized by MALDI-TOF MS.

Preparation of Tag-Free Macrocycles. Tag-free macrocycles were produced by proteolytic cleavage of the CBD tag with Factor Xa or thiol-induced cleavage of the GyrA tag. For cleavage of the CBD tag, the purified CBD-fused macrocycles (250 μM) were digested with 5 μg/mL of Factor Xa protease (NEB) in Factor Xa buffer (20 mM Tris, 100 mM NaCl, 2 mM CaCl2, pH = 8.0) overnight at room temperature. The reaction was acidified with TFA (0.1%) and purified by solid-phase extraction with a step gradient of acetonitrile in water (+0.1% TFA). Fractions containing peptide were lyophilized, and peptide identity was confirmed by MALDI-TOF MS. For cleavage of the GyrA intein tag, the purified GyrA-fused macrocycles (∼200 μM) were incubated in potassium phosphate buffer (10 mM potassium phosphate, 150 mM NaCl, pH 8.5) containing 20 mM TCEP (tris(2-carboxyethyl) phosphine) and 10 mM thiophenol, for 16 h at room temperature with gentle shaking. The solutions were then dialyzed against water to remove excess thiophenol, and then acidified with 0.1% TFA. The cleaved peptide was purified via solid-phase extraction with a step gradient of acetonitrile in water (+0.1% TFA). After lyophilization, the peptide identity was reconfirmed by MALDI-TOF MS.

Binding Assays. For the streptavidin-binding assays, streptavidin-coated plates (Sigma-Aldrich) were used. For the Shh- and Keap1-binding assays, either Shh or Keap1 was immobilized on microtiter plates by incubating 100 μL of a 4 μM protein solution in PBS buffer overnight at 4 °C, followed by washing (3 × 150 μL of PBS with 0.5% Tween-20) and blocking with 0.5% bovine serum albumin in PBS for 1.5 h at room temperature. After washing, each well was incubated with 100 μL of purified FLAG-tagged peptide at varying concentrations for 1 h at room temperature. After washing three times with wash buffer, each well was incubated with 100 μL of a 1:2500 dilution of HRP-conjugate mouse anti-FLAG polyclonal antibody (Sigma-Aldrich) for 1 h at room temperature. After three washing steps with wash buffer, 100 μL of 2.2 mM o-phenylenediamine dihydrochloride, 4.2 mM urea hydrogen peroxide, 100 mM dibasic sodium phosphate, and 50 mM sodium citrate, pH 5.0, was added to each well, followed by measurement of the absorbance at 450 nm after 10−20 min using a Tecan Infinite 1000 plate reader. Equilibrium dissociation constants (K_D) were determined by fitting the dose−response curves to a 1:1 binding isotherm equation via nonlinear regression using SigmaPlot. Mean values and standard deviations were calculated from experiments performed in triplicate.

Keap1 Competition Assay. Keap1 was immobilized on microtiter plates as described above. After washing, each well was incubated for 1 h at room temperature with 100 μL of serial dilutions of a peptide corresponding to $Nrf2_{77-83}$ (Ac-DEETGEF−OH) in PBS buffer containing 800 nM FLAG-tagged KKD-m1. After washing, the bound peptide was quantified by means of HRP-conjugate mouse anti-FLAG polyclonal antibody and colorimetric assay as described above. The inhibitory constant (IC_{50}) was determined by fitting the dose−response curves to a 4-parameter equation via nonlinear regression using SigmaPlot. Mean values and standard deviations were calculated from experiments performed in triplicate.

Shh Competition Assay. Shh-GST was immobilized on microtiter plates as described above. After washing, each well was incubated for 1 h at room temperature with 100 μL of a solution of the FLAG-tagged peptide (Shh-m1, Shh-m2, or Shh(6X)-m2) at 1 μM in PBS buffer, also containing 200 μM robotnikinin. No inhibitor control wells were prepared without adding robotnikinin. After washing three times with wash buffer, each well was incubated with 100 μL of a 1:2500 dilution of HRP-conjugate mouse anti-FLAG polyclonal antibody (Sigma-Aldrich) for 1 h at room temperature. After washing, the bound peptide was quantified by means of HRP-conjugate mouse anti-FLAG polyclonal antibody and colorimetric assay as described above. The percent peptide bound was normalized to the response of the no-inhibitor control wells. Mean values and standard deviations were calculated from experiments performed in triplicate.

■ ASSOCIATED CONTENT

Supporting Information

The Supporting Information is available free of charge at https://pubs.acs.org/doi/10.1021/acscentsci.9b00927.

Supporting figures, oligonucleotide sequences, and MS spectra (PDF)

■ AUTHOR INFORMATION

Corresponding Author

Rudi Fasan − *Department of Chemistry, University of Rochester, Rochester, New York 14627, United States;* orcid.org/0000-0003-4636-9578; Email: rfasan@ur.rochester.edu

Authors

Andrew E. Owens − *Department of Chemistry, University of Rochester, Rochester, New York 14627, United States*

Jacob A. Iannuzzelli − *Department of Chemistry, University of Rochester, Rochester, New York 14627, United States*

Yu Gu − *Department of Chemistry, University of Rochester, Rochester, New York 14627, United States*

Complete contact information is available at: https://pubs.acs.org/10.1021/acscentsci.9b00927

Author Contributions

†A.E.O. and J.A.I. contributed equally to this work.

Notes

The authors declare the following competing financial interest(s): Results of this work are part of a patent application filed by the University of Rochester.

■ ACKNOWLEDGMENTS

We are grateful to Prof. Adrian Whitty (Boston University) for providing a plasmid for the expression of Keap1 and Dr. John R. Frost for synthesizing the biot-Cys reagent. This research was supported by the U.S. National Institute of Health grant R01 GM134076. MS instrumentation at the University of Rochester was supported by the National Science Foundation grants CHE-0840410 and CHE-0946653.

REFERENCES

(1) Driggers, E. M.; Hale, S. P.; Lee, J.; Terrett, N. K. The exploration of macrocycles for drug discovery–an underexploited structural class. *Nat. Rev. Drug Discovery* **2008**, *7*, 608−624.

(2) Robinson, J. A.; Demarco, S.; Gombert, F.; Moehle, K.; Obrecht, D. The design, structures and therapeutic potential of protein epitope mimetics. *Drug Discovery Today* **2008**, *13*, 944−951.

(3) Marsault, E.; Peterson, M. L. Macrocycles are great cycles: applications, opportunities, and challenges of synthetic macrocycles in drug discovery. *J. Med. Chem.* **2011**, *54*, 1961−2004.

(4) Hill, T. A.; Shepherd, N. E.; Diness, F.; Fairlie, D. P. Constraining cyclic peptides to mimic protein structure motifs. *Angew. Chem., Int. Ed.* **2014**, *53*, 13020−13041.

(5) Valeur, E.; Gueret, S. M.; Adihou, H.; Gopalakrishnan, R.; Lemurell, M.; Waldmann, H.; Grossmann, T. N.; Plowright, A. T. New modalities for challenging targets in drug discovery. *Angew. Chem., Int. Ed.* **2017**, *56*, 10294−10323.

(6) Cardote, T. A.; Ciulli, A. Cyclic and macrocyclic peptides as chemical tools to recognise protein surfaces and probe protein-protein Interactions. *ChemMedChem* **2016**, *11*, 787−794.

(7) Villar, E. A.; Beglov, D.; Chennamadhavuni, S.; Porco, J. A., Jr.; Kozakov, D.; Vajda, S.; Whitty, A. How proteins bind macrocycles. *Nat. Chem. Biol.* **2014**, *10*, 723−731.

(8) Malde, A. K.; Hill, T. A.; Iyer, A.; Fairlie, D. P. Crystal structures of protein-bound cyclic peptides. *Chem. Rev.* **2019**, *119*, 9861−9914.

(9) Fairlie, D. P.; Tyndall, J. D.; Reid, R. C.; Wong, A. K.; Abbenante, G.; Scanlon, M. J.; March, D. R.; Bergman, D. A.; Chai, C. L.; Burkett, B. A. Conformational selection of inhibitors and substrates by proteolytic enzymes: implications for drug design and polypeptide processing. *J. Med. Chem.* **2000**, *43*, 1271−1281.

(10) Wang, D.; Liao, W.; Arora, P. S. Enhanced metabolic stability and protein-binding properties of artificial alpha helices derived from a hydrogen-bond surrogate: application to Bcl-xL. *Angew. Chem., Int. Ed.* **2005**, *44*, 6525−6529.

(11) Lesniak, W. G.; Aboye, T.; Chatterjee, S.; Camarero, J. A.; Nimmagadda, S. In vivo evaluation of an engineered cyclotide as specific CXCR4 imaging reagent. *Chem. - Eur. J.* **2017**, *23*, 14469−14475.

(12) Aboye, T. L.; Ha, H.; Majumder, S.; Christ, F.; Debyser, Z.; Shekhtman, A.; Neamati, N.; Camarero, J. A. Design of a novel cyclotide-based CXCR4 antagonist with anti-human immunodeficiency virus (HIV)-1 activity. *J. Med. Chem.* **2012**, *55*, 10729−10734.

(13) Walensky, L. D.; Kung, A. L.; Escher, I.; Malia, T. J.; Barbuto, S.; Wright, R. D.; Wagner, G.; Verdine, G. L.; Korsmeyer, S. J. Activation of apoptosis in vivo by a hydrocarbon-stapled BH3 helix. *Science* **2004**, *305*, 1466−1470.

(14) Ji, Y. B.; Majumder, S.; Millard, M.; Borra, R.; Bi, T.; Elnagar, A. Y.; Neamati, N.; Shekhtman, A.; Camarero, J. A. In Vivo Activation of the p53 Tumor Suppressor Pathway by an Engineered Cyclotide. *J. Am. Chem. Soc.* **2013**, *135*, 11623−11633.

(15) Nielsen, D. S.; Hoang, H. N.; Lohman, R. J.; Hill, T. A.; Lucke, A. J.; Craik, D. J.; Edmonds, D. J.; Griffith, D. A.; Rotter, C. J.; Ruggeri, R. B.; Price, D. A.; Liras, S.; Fairlie, D. P. Improving on nature: making a cyclic heptapeptide orally bioavailable. *Angew. Chem., Int. Ed.* **2014**, *53*, 12059−12063.

(16) Hewitt, W. M.; Leung, S. S. F.; Pye, C. R.; Ponkey, A. R.; Bednarek, M.; Jacobson, M. P.; Lokey, R. S. Cell-permeable cyclic peptides from synthetic libraries inspired by natural products. *J. Am. Chem. Soc.* **2015**, *137*, 715−721.

(17) Wu, H.; Mousseau, G.; Mediouni, S.; Valente, S. T.; Kodadek, T. Cell-permeable peptides containing cycloalanine residues. *Angew. Chem., Int. Ed.* **2016**, *55*, 12637−12642.

(18) Furukawa, A.; Townsend, C. E.; Schwochert, J.; Pye, C. R.; Bednarek, M. A.; Lokey, R. S. Passive membrane permeability in cyclic peptomer scaffolds is robust to extensive variation in side chain functionality and backbone geometry. *J. Med. Chem.* **2016**, *59*, 9503−9512.

(19) Peraro, L.; Zou, Z. J.; Makwana, K. M.; Cummings, A. E.; Ball, H. L.; Yu, H. T.; Lin, Y. S.; Levine, B.; Kritzer, J. A. Diversity-oriented stapling yields intrinsically cell-penetrant inducers of autophagy. *J. Am. Chem. Soc.* **2017**, *139*, 7792−7802.

(20) Nawatha, M.; Rogers, J. M.; Bonn, S. M.; Livneh, I.; Lemma, B.; Mali, S. M.; Vamisetti, G. B.; Sun, H.; Bercovich, B.; Huang, Y. C.; Ciechanover, A.; Fushman, D.; Suga, H.; Brik, A. De novo macrocyclic peptides that specifically modulate Lys48-linked ubiquitin chains. *Nat. Chem.* **2019**, *11*, 644−652.

(21) Smith, G. P.; Petrenko, V. A. Phage display. *Chem. Rev.* **1997**, *97*, 391−410.

(22) Ladner, R. C.; Sato, A. K.; Gorzelany, J.; de Souza, M. Phage display-derived peptides as therapeutic alternatives to antibodies. *Drug Discovery Today* **2004**, *9*, 525−529.

(23) Josephson, K.; Ricardo, A.; Szostak, J. W. mRNA display: from basic principles to macrocycle drug discovery. *Drug Discovery Today* **2014**, *19*, 388−399.

(24) Angelini, A.; Heinis, C. Post-translational modification of genetically encoded polypeptide libraries. *Curr. Opin. Chem. Biol.* **2011**, *15*, 355−361.

(25) Horswill, A. R.; Benkovic, S. J. Cyclic peptides, a chemical genetics tool for biologists. *Cell Cycle* **2005**, *4*, 552−555.

(26) Tavassoli, A. SICLOPPS cyclic peptide libraries in drug discovery. *Curr. Opin. Chem. Biol.* **2017**, *38*, 30−35.

(27) Passioura, T.; Katoh, T.; Goto, Y.; Suga, H. Selection-based discovery of druglike macrocyclic peptides. *Annu. Rev. Biochem.* **2014**, *83*, 727−752.

(28) Frost, J. R.; Smith, J. M.; Fasan, R. Design, synthesis, and diversification of ribosomally derived peptide macrocycles. *Curr. Opin. Struct. Biol.* **2013**, *23*, 571−580.

(29) Hetrick, K. J.; Walker, M. C.; van der Donk, W. A. Development and application of yeast and phage display of diverse lanthipeptides. *ACS Cent. Sci.* **2018**, *4*, 458−467.

(30) Sidhu, S. S.; Lowman, H. B.; Cunningham, B. C.; Wells, J. A. Phage display for selection of novel binding peptides. *Methods Enzymol.* **2000**, *328*, 333−363.

(31) Clackson, T.; Wells, J. A. A hot spot of binding energy in a hormone-receptor interface. *Science* **1995**, *267*, 383−386.

(32) Meyer, S. C.; Shomin, C. D.; Gaj, T.; Ghosh, I. Tethering small molecules to a phage display library: discovery of a selective bivalent inhibitor of protein kinase A. *J. Am. Chem. Soc.* **2007**, *129*, 13812−13813.

(33) Heinis, C.; Winter, G. Encoded libraries of chemically modified peptides. *Curr. Opin. Chem. Biol.* **2015**, *26*, 89−98.

(34) Rentero Rebollo, I.; Heinis, C. Phage selection of bicyclic peptides. *Methods* **2013**, *60*, 46−54.

(35) Howell, S. M.; Fiacco, S. V.; Takahashi, T. T.; Jalali-Yazdi, F.; Millward, S. W.; Hu, B. L.; Wang, P.; Roberts, R. W. Serum stable natural peptides designed by mRNA display. *Sci. Rep.* **2015**, *4*, 6008.

(36) Nichols, A. L.; Noridomi, K.; Hughes, C. R.; Jalali-Yazdi, F.; Eaton, J. B.; Lai, L. H.; Advani, G.; Lukas, R. J.; Lester, H. A.; Chen, L.; Roberts, R. W. alpha 1-FANGs: Protein ligands selective for the alpha-bungarotoxin site of the alpha 1-nicotinic acetylcholine receptor. *ACS Chem. Biol.* **2018**, *13*, 2568−2576.

(37) White, E. R.; Sun, L. X.; Ma, Z.; Beckta, J. M.; Danzig, B. A.; Hacker, D. E.; Huie, M.; Williams, D. C.; Edwards, R. A.; Valerie, K.; Glover, J. N. M.; Hartman, M. C. T. Peptide library approach to uncover phosphomimetic inhibitors of the BRCA1 C-terminal domain. *ACS Chem. Biol.* **2015**, *10*, 1198−1208.

(38) Hipolito, C. J.; Suga, H. Ribosomal production and in vitro selection of natural product-like peptidomimetics: The FIT and RaPID systems. *Curr. Opin. Chem. Biol.* **2012**, *16*, 196−203.

(39) Kawamura, A.; Munzel, M.; Kojima, T.; Yapp, C.; Bhushan, B.; Goto, Y.; Tumber, A.; Katoh, T.; King, O. N. F.; Passioura, T.; Walport, L. J.; Hatch, S. B.; Madden, S.; Muller, S.; Brennan, P. E.; Chowdhury, R.; Hopkinson, R. J.; Suga, H.; Schofield, C. J. Highly selective inhibition of histone demethylases by de novo macrocyclic peptides. *Nat. Commun.* **2017**, *8*, 14773.

(40) Horswill, A. R.; Savinov, S. N.; Benkovic, S. J. A systematic method for identifying small-molecule modulators of protein-protein interactions. *Proc. Natl. Acad. Sci. U. S. A.* **2004**, *101*, 15591−15596.

https://dx.doi.org/10.1021/acscentsci.9b00927
ACS Cent. Sci. 2020, 6, 368−381

(41) Tavassoli, A.; Benkovic, S. J. Genetically selected cyclic-peptide inhibitors of AICAR transformylase homodimerization. *Angew. Chem., Int. Ed.* **2005**, *44*, 2760−2763.
(42) Tavassoli, A.; Lu, Q.; Gam, J.; Pan, H.; Benkovic, S. J.; Cohen, S. N. Inhibition of HIV budding by a genetically selected cyclic peptide targeting the Gag-TSG101 interaction. *ACS Chem. Biol.* **2008**, *3*, 757−764.
(43) Miranda, E.; Nordgren, I. K.; Male, A. L.; Lawrence, C. E.; Hoakwie, F.; Cuda, F.; Court, W.; Fox, K. R.; Townsend, P. A.; Packham, G. K.; Eccles, S. A.; Tavassoli, A. A cyclic peptide inhibitor of HIF-1 heterodimerization that inhibits hypoxia signaling in cancer cells. *J. Am. Chem. Soc.* **2013**, *135*, 10418−10425.
(44) Wrighton, N. C.; Farrell, F. X.; Chang, R.; Kashyap, A. K.; Barbone, F. P.; Mulcahy, L. S.; Johnson, D. L.; Barrett, R. W.; Jolliffe, L. K.; Dower, W. J. Small peptides as potent mimics of the protein hormone erythropoietin. *Science* **1996**, *273*, 458−463.
(45) Lowman, H. B.; Chen, Y. M.; Skelton, N. J.; Mortensen, D. L.; Tomlinson, E. E.; Sadick, M. D.; Robinson, I. C.; Clark, R. G. Molecular mimics of insulin-like growth factor 1 (IGF-1) for inhibiting IGF-1: IGF-binding protein interactions. *Biochemistry* **1998**, *37*, 8870−8878.
(46) Fairbrother, W. J.; Christinger, H. W.; Cochran, A. G.; Fuh, G.; Keenan, C. J.; Quan, C.; Shriver, S. K.; Tom, J. Y.; Wells, J. A.; Cunningham, B. C. Novel peptides selected to bind vascular endothelial growth factor target the receptor-binding site. *Biochemistry* **1998**, *37*, 17754−17764.
(47) Nakamura, G. R.; Reynolds, M. E.; Chen, Y. M.; Starovasnik, M. A.; Lowman, H. B. Stable "zeta" peptides that act as potent antagonists of the high-affinity IgE receptor. *Proc. Natl. Acad. Sci. U. S. A.* **2002**, *99*, 1303−1308.
(48) Eckert, D. M.; Malashkevich, V. N.; Hong, L. H.; Carr, P. A.; Kim, P. S. Inhibiting HIV-1 entry: discovery of D-peptide inhibitors that target the gp41 coiled-coil pocket. *Cell* **1999**, *99*, 103−115.
(49) DeLano, W. L.; Ultsch, M. H.; de Vos, A. M.; Wells, J. A. Convergent solutions to binding at a protein-protein interface. *Science* **2000**, *287*, 1279−1283.
(50) Dias, R. L.; Fasan, R.; Moehle, K.; Renard, A.; Obrecht, D.; Robinson, J. A. Protein ligand design: from phage display to synthetic protein epitope mimetics in human antibody Fc-binding peptidomimetics. *J. Am. Chem. Soc.* **2006**, *128*, 2726−2732.
(51) Quartararo, J. S.; Wu, P.; Kritzer, J. A. Peptide bicycles that inhibit the Grb2 SH2 domain. *ChemBioChem* **2012**, *13*, 1490−1496.
(52) Heinis, C.; Rutherford, T.; Freund, S.; Winter, G. Phage-encoded combinatorial chemical libraries based on bicyclic peptides. *Nat. Chem. Biol.* **2009**, *5*, 502−507.
(53) Angelini, A.; Cendron, L.; Chen, S. Y.; Touati, J.; Winter, G.; Zanotti, G.; Heinis, C. Bicyclic peptide inhibitor reveals large contact interface with a protease target. *ACS Chem. Biol.* **2012**, *7*, 817−821.
(54) Baeriswyl, V.; Calzavarini, S.; Chen, S. Y.; Zorzi, A.; Bologna, L.; Angelillo-Scherrer, A.; Heinis, C. A synthetic factor XIIa inhibitor blocks selectively intrinsic coagulation initiation. *ACS Chem. Biol.* **2015**, *10*, 1861−1870.
(55) Baeriswyl, V.; Calzavarini, S.; Gerschheimer, C.; Diderich, P.; Angelillo-Scherrer, A.; Heinis, C. Development of a selective peptide macrocycle inhibitor of coagulation factor XII toward the generation of a safe antithrombotic therapy. *J. Med. Chem.* **2013**, *56*, 3742−3746.
(56) Ng, S.; Derda, R. Phage-displayed macrocyclic glycopeptide libraries. *Org. Biomol. Chem.* **2016**, *14*, 5539−5545.
(57) Urban, J. H.; Moosmeier, M. A.; Aumuller, T.; Thein, M.; Bosma, T.; Rink, R.; Groth, K.; Zulley, M.; Siegers, K.; Tissot, K.; Moll, G. N.; Prassler, J. Phage display and selection of lanthipeptides on the carboxy-terminus of the gene-3 minor coat protein. *Nat. Commun.* **2017**, *8*, 1500.
(58) Smith, J. M.; Vitali, F.; Archer, S. A.; Fasan, R. Modular assembly of Macrocyclic Organo-Peptide Hybrids using synthetic and genetically encoded precursors. *Angew. Chem., Int. Ed.* **2011**, *50*, 5075−5080.
(59) Satyanarayana, M.; Vitali, F.; Frost, J. R.; Fasan, R. Diverse organo-peptide macrocycles via a fast and catalyst-free oxime/intein-mediated dual ligation. *Chem. Commun.* **2012**, *48*, 1461−1463.
(60) Frost, J. R.; Jacob, N. T.; Papa, L. J.; Owens, A. E.; Fasan, R. Ribosomal synthesis of macrocyclic peptides in vitro and in vivo mediated by genetically encoded aminothiol unnatural amino acids. *ACS Chem. Biol.* **2015**, *10*, 1805−1816.
(61) Bionda, N.; Cryan, A. L.; Fasan, R. Bioinspired strategy for the ribosomal synthesis of thioether-bridged macrocyclic peptides in bacteria. *ACS Chem. Biol.* **2014**, *9*, 2008−2013.
(62) Bionda, N.; Fasan, R. Ribosomal synthesis of natural product-like bicyclic peptides in *Escherichia coli*. *ChemBioChem* **2015**, *16*, 2011−2016.
(63) Owens, A. E.; de Paola, I.; Hansen, W. A.; Liu, Y. W.; Khare, S. D.; Fasan, R. Design and evolution of a macrocyclic peptide inhibitor of the Sonic Hedgehog/Patched interaction. *J. Am. Chem. Soc.* **2017**, *139*, 12559−12568.
(64) Rondot, S.; Koch, J.; Breitling, F.; Dubel, S. A helper phage to improve single-chain antibody presentation in phage display. *Nat. Biotechnol.* **2001**, *19*, 75−78.
(65) Broders, O.; Breitling, F.; Dubel, S. Hyperphage. Improving antibody presentation in phage display. *Methods Mol. Biol.* **2002**, *205*, 295−302.
(66) Rulker, T.; Voss, L.; Thullier, P.; O'Brien, L. M.; Pelat, T.; Perkins, S. D.; Langermann, C.; Schirrmann, T.; Dubel, S.; Marschall, H. J.; Hust, M.; Hulseweh, B. Isolation and characterisation of a human-like antibody fragment (scFv) that inactivates VEEV in vitro and in vivo. *PLoS One* **2012**, *7*, No. e37242.
(67) Tian, F.; Tsao, M.-L.; Schultz, P. G. A phage display system with unnatural amino acids. *J. Am. Chem. Soc.* **2004**, *126*, 15962−15963.
(68) Liu, C. C.; Mack, A. V.; Tsao, M. L.; Mills, J. H.; Lee, H. S.; Choe, H.; Farzan, M.; Schultz, P. G.; Smider, V. V. Protein evolution with an expanded genetic code. *Proc. Natl. Acad. Sci. U. S. A.* **2008**, *105*, 17688−17693.
(69) Liu, C. C.; Schultz, P. G. Adding new chemistries to the genetic code. *Annu. Rev. Biochem.* **2010**, *79*, 413−444.
(70) Wang, L.; Xie, J.; Schultz, P. G. Expanding the genetic code. *Annu. Rev. Biophys. Biomol. Struct.* **2006**, *35*, 225−249.
(71) Young, T. S.; Ahmad, I.; Yin, J. A.; Schultz, P. G. An enhanced system for unnatural amino acid mutagenesis in E. coli. *J. Mol. Biol.* **2010**, *395*, 361−374.
(72) Weber, P. C.; Pantoliano, M. W.; Thompson, L. D. Crystal-structure and ligand-binding studies of a screened peptide complexed with streptavidin. *Biochemistry* **1992**, *31*, 9350−9354.
(73) Giebel, L. B.; Cass, R. T.; Milligan, D. L.; Young, D. C.; Arze, R.; Johnson, C. R. Screening of cyclic peptide phage libraries identifies ligands that bind streptavidin with high affinities. *Biochemistry* **1995**, *34*, 15430−15435.
(74) Katz, B. A. Structural and mechanistic determinants of affinity and specificity of ligands discovered or engineered by phage display. *Annu. Rev. Biophys. Biomol. Struct.* **1997**, *26*, 27−45.
(75) Katz, B. A. Binding to protein targets of peptidic leads discovered by phage display - Crystal-structures of streptavidin-bound linear and cyclic peptide ligands containing the HPQ sequence. *Biochemistry* **1995**, *34*, 15421−15429.
(76) Itoh, K.; Wakabayashi, N.; Katoh, Y.; Ishii, T.; Igarashi, K.; Engel, J. D.; Yamamoto, M. Keap1 represses nuclear activation of antioxidant responsive elements by Nrf2 through binding to the amino-terminal Neh2 domain. *Genes Dev.* **1999**, *13*, 76−86.
(77) Dhakshinamoorthy, S.; Jaiswal, A. K. Functional characterization and role of INrf2 in antioxidant response element-mediated expression and antioxidant induction of NAD(P)H:quinone oxidoreductase1 gene. *Oncogene* **2001**, *20*, 3906−3917.
(78) Zhang, D. D.; Hannink, M. Distinct cysteine residues in Keap1 are required for Keap1-dependent ubiquitination of Nrf2 and for stabilization of Nrf2 by chemopreventive agents and oxidative stress. *Mol. Cell. Biol.* **2003**, *23*, 8137−8151.

(79) Thimmulappa, R. K.; Fuchs, R. J.; Malhotra, D.; Scollick, C.; Traore, K.; Bream, J. H.; Trush, M. A.; Liby, K. T.; Sporn, M. B.; Kensler, T. W.; Biswali, S. Preclinical evaluation of targeting the Nrf2 pathway by triterpenoids (CDDO-Im and CDDO-Me) for protection from LPS-induced inflammatory response and reactive oxygen species in human peripheral blood mononuclear cells and neutrophils. *Antioxid. Redox Signaling* **2007**, *9*, 1963−1970.
(80) Steel, R.; Cowan, J.; Payerne, E.; O'Connell, M. A.; Searcey, M. Anti-inflammatory Effect of a Cell-Penetrating Peptide Targeting the Nrf2/Keap1 Interaction. *ACS Med. Chem. Lett.* **2012**, *3*, 407−410.
(81) Pergola, P. E.; Raskin, P.; Toto, R. D.; Meyer, C. J.; Huff, J. W.; Grossman, E. B.; Krauth, M.; Ruiz, S.; Audhya, P.; Christ-Schmidt, H.; Wittes, J.; Warnock, D. G. Bardoxolone methyl and kidney function in CKD with Type 2 diabetes. *N. Engl. J. Med.* **2011**, *365*, 327−336.
(82) Sandberg, M.; Patil, J.; D'Angelo, B.; Weber, S. G.; Mallard, C. NRF2-regulation in brain health and disease: Implication of cerebral inflammation. *Neuropharmacology* **2014**, *79*, 298−306.
(83) Lo, S. C.; Li, X. C.; Henzl, M. T.; Beamer, L. J.; Hannink, M. Structure of the Keap1: Nrf2 interface provides mechanistic insight into Nrf2 signaling. *EMBO J.* **2006**, *25*, 3605−3617.
(84) Hancock, R.; Schaap, M.; Pfister, H.; Wells, G. Peptide inhibitors of the Keap1-Nrf2 protein-protein interaction with improved binding and cellular activity. *Org. Biomol. Chem.* **2013**, *11*, 3553−3557.
(85) Chiang, C.; Ying, L. T. T.; Lee, E.; Young, K. E.; Corden, J. L.; Westphal, H.; Beachy, P. A. Cyclopia and defective axial patterning in mice lacking Sonic hedgehog gene function. *Nature* **1996**, *383*, 407−413.
(86) Ingham, P. W.; McMahon, A. P. Hedgehog signaling in animal development: paradigms and principles. *Genes Dev.* **2001**, *15*, 3059−3087.
(87) Ingham, P. W.; Placzek, M. Orchestrating ontogenesis: variations on a theme by sonic hedgehog. *Nat. Rev. Genet.* **2006**, *7*, 841−850.
(88) Rubin, L. L.; de Sauvage, F. J. Targeting the Hedgehog pathway in cancer. *Nat. Rev. Drug Discovery* **2006**, *5*, 1026−1033.
(89) Theunissen, J. W.; de Sauvage, F. J. Paracrine Hedgehog signaling in cancer. *Cancer Res.* **2009**, *69*, 6007−6010.
(90) Carpenter, D.; Stone, D. M.; Brush, J.; Ryan, A.; Armanini, M.; Frantz, G.; Rosenthal, A.; de Sauvage, F. J. Characterization of two patched receptors for the vertebrate hedgehog protein family. *Proc. Natl. Acad. Sci. U. S. A.* **1998**, *95*, 13630−13634.
(91) Denef, N.; Neubuser, D.; Perez, L.; Cohen, S. M. Hedgehog induces opposite changes in turnover and subcellular localization of patched and smoothened. *Cell* **2000**, *102*, 521−531.
(92) Yoon, J. W.; Kita, Y.; Frank, D. J.; Majewski, R. R.; Konicek, B. A.; Nobrega, M. A.; Jacob, H.; Walterhouse, D.; Iannaccone, P. Gene expression profiling leads to identification of GLI1-binding elements in target genes and a role for multiple downstream pathways in GLI1-induced cell transformation. *J. Biol. Chem.* **2002**, *277*, 5548−5555.
(93) Kasper, M.; Regl, G.; Frischauf, A. M.; Aberger, F. GLI transcription factors: mediators of oncogenic Hedgehog signalling. *Eur. J. Cancer* **2006**, *42*, 437−445.
(94) Bosanac, I.; Maun, H. R.; Scales, S. J.; Wen, X.; Lingel, A.; Bazan, J. F.; de Sauvage, F. J.; Hymowitz, S. G.; Lazarus, R. A. The structure of SHH in complex with HHIP reveals a recognition role for the Shh pseudo active site in signaling. *Nat. Struct. Mol. Biol.* **2009**, *16*, 691−697.
(95) Bishop, B.; Aricescu, A. R.; Harlos, K.; O'Callaghan, C. A.; Jones, E. Y.; Siebold, C. Structural insights into hedgehog ligand sequestration by the human hedgehog-interacting protein HHIP. *Nat. Struct. Mol. Biol.* **2009**, *16*, 698−U629.
(96) Chuang, P. T.; McMahon, A. P. Vertebrate Hedgehog signalling modulated by induction of a Hedgehog-binding protein. *Nature* **1999**, *397*, 617−621.
(97) Gong, X.; Qian, H.; Cao, P.; Zhao, X.; Zhou, Q.; Lei, J.; Yan, N. Structural basis for the recognition of Sonic Hedgehog by human Patched1. *Science* **2018**, *361*, eaas8935.
(98) Qi, X. F.; Schmiege, P.; Coutavas, E.; Wang, J. W.; Li, X. C. Structures of human Patched and its complex with native palmitoylated sonic hedgehog. *Nature* **2018**, *560*, 128−132.
(99) Stanton, B. Z.; Peng, L. F.; Maloof, N.; Nakai, K.; Wang, X.; Duffner, J. L.; Taveras, K. M.; Hyman, J. M.; Lee, S. W.; Koehler, A. N.; Chen, J. K.; Fox, J. L.; Mandinova, A.; Schreiber, S. L. A small molecule that binds Hedgehog and blocks its signaling in human cells. *Nat. Chem. Biol.* **2009**, *5*, 154−156.
(100) Horer, S.; Reinert, D.; Ostmann, K.; Hoevels, Y.; Nar, H. Crystal-contact engineering to obtain a crystal form of the Kelch domain of human Keap1 suitable for ligand-soaking experiments. *Acta Crystallogr., Sect. F: Struct. Biol. Cryst. Commun.* **2013**, *69*, 592−596.

https://dx.doi.org/10.1021/acscentsci.9b00927
ACS Cent. Sci. 2020, 6, 368−381